XLI CILAMCE
XLI Ibero-Latin American Congress on Computational Methods in Engineering
16-19 November, 2020 FOZ DO IGUAÇU PARANÁ - BRAZIL

Computational modeling of formation and evolution of damage zones in reservoir scale

Thiago J. de Andrade[1,2], Roberto Quevedo[2], Bruno R.B.M. Carvalho[3], Deane Roehl[1,2]

[1]*Civil and Environmental Engineering Department, PUC-Rio*
Rua Marquês de São Vicente, 225, 22453-900, Rio de Janeiro, Brazil
juvencio@aluno.puc-rio.br, droehl@puc-rio.br
[2]*Tecgraf Institute, PUC-Rio*
Rua Marquês de São Vicente, 225, 22453-900, Rio de Janeiro, Brazil
thiagojuvencio@tecgraf.puc-rio.br, rquevedo@tecgraf.puc-rio.br, deane@tecgraf.puc-rio.br
[3]*Petrobras Research Center*
Av. Horácio Macedo, 950, 21941-915, Rio de Janeiro, Brazil
brcarvalho@petrobras.com.br

Abstract. Geological fault zones can act as barriers or conducts for oil and gas flow in petroleum reservoirs. Fault zones are divided into two regions, the fault core and the adjacent damage zone. The core is the region that concentrates the greatest displacement and in general acts as a barrier for fluid-flow. On the other hand, damage zones are characterized by relatively less intense deformation and can exhibit geological structures such as fractures and deformation bands. Such zones can impact not only the fluid-flow within the reservoir but also the mechanical behavior. Thus, the characterization of the damage zones is crucial for better management of oil fields during the production phase. In this study, we present numerical models based on the finite element method (FEM) to study the structural evolution of the damage zones in reservoir scale. Sensitivity analyzes were performed varying the mechanical properties of intact rocks in order to check their impact on the structural evolution of the damage zone. The obtained results allowed the identification of key parameters for damage zone evolution and highlighted some advantages of FEM for the analysis of this kind of process.

Keywords: Damage zones, Fault, Numerical modelling, Finite element method, Plasticity.

1 Introduction

Geological faults are common and important in many types of basins around the world and are responsible for the compartmentalization of most reservoirs in the oil and gas fields. Such compartmentalization could occur as a consequence of the core, which is responsible for avoiding fluid-flow across the fault, giving the fault a sealing feature [1][2]. Traditionally, in the oil and gas industry, geological faults have been considered as planes owing to the seismic acquisition resolution in deep formations. However, field observations in outcrops demonstrate that geological faults are not simple planes, but complex geological structures which can trigger positive or even extremely negative impacts on fluid-flow within reservoirs [1]. For this reason, the term “fault zone” has been used more appropriately to designate the entire region where the deformation is concentrated [2].

A fault zone can contain high-strain zones, where the core develops, and low-strain zones surrounding the core, commonly referred to as “damage zones”. Figure 1 shows a representative fault zone in the reservoir scale. Damage zones may include a wide diversity of geological structures such as deformation bands (dilation, shear and compaction bands), tensile fractures, fault-related folds and/or smaller faults [3]. The different deformation mechanisms can be attributed to the lithology, mechanical properties (elastic and strength), petrophysical properties (porosity) and the stress state of the host rock under deformation [4][5]. In general, porous rocks, such as sandstones, with lower stiffness in comparison to low-porosity rocks, respond to stress changes by grain reorganization and breakage, resulting in different types of deformation bands. On the other hand, low-porosity

rocks, such as carbonates, usually respond to stress changes by fracturing [5]. These geological structures may trigger significant and variable impacts on the rock permeability [4]. For example, if fractures are dominant, the damage zone may act as a conduit, while if deformation bands or veins (mineral-filled fractures) are dominant, damage zones act as barriers [6].

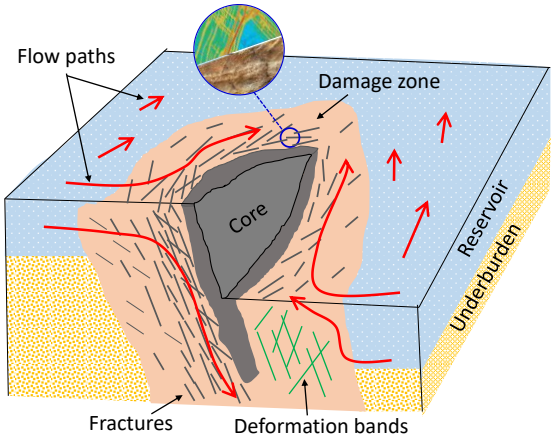

Figure 1. Schematic illustration of a fault zone, with the representation of fault core and damage zone

Despite their importance for hydrocarbon production, the characterization of damage zones remains poorly explored and still under debate [4]. An approach usually adopted to characterize the damage zone structure consists of field observations in outcrops [3]. Due to the extreme variability of geological features around fault zones, some researchers [5][7][8] have used the cumulative frequency of deformation bands and fractures around the fault core to define the damage zone width. Moreover, from outcrops, it is possible to measure fault displacements through visual inspection. As a result, scaling relationships (mainly power-law) between fault displacement and damage-zone width have been proposed in the literature [4][9][10]. Those relationships are very important since fault displacements can be captured in seismic acquisitions, and hence, geoscientists can be aware of the damage zone width. However, damage zones depend on several factors, including mechanical and petrophysical properties of the rock formation.

Another option for the characterization of damage zones is to perform laboratory tests on analogue rock samples and inducing the fault zone through shear tests [11]. Nonetheless, those tests only can be performed in reduced scales, which are not representative of reservoir scales. Another alternative for damage zone characterization is numerical modeling. Numerical models, particularly FEM, can be excellent tools for the understanding of the structural evolution of damage zones. Furthermore, FEM can deal with non-linear friction/plastic materials and consider irregular geometries and complex boundary conditions such as frictional boundaries [12][13].

In this study, we present numerical models based on the FEM to study the structural evolution of the damage zones of normal faults in carbonate rocks in the reservoir scale. Sensitivity analyzes were performed varying elastic and strength properties as well as in-situ stresses in order to check their impact on the structural evolution of the damage zone. The obtained results allowed to identify key parameters for the development of damage zones. Furthermore, we also discuss the advantages and limitations of FEM for modeling this kind of problem.

2 Model description

In this section, we describe the numerical model used to simulate the structural evolution of damage zones in the reservoir scale. The model setting, presented in Fig. 2, is based on [14] and focuses on deformation localization in normal faults under plane-strain conditions. The mechanical behavior of the rock was represented through an elastoplastic model, using the Mohr-Coulomb failure criterion with non-associative plastic flow law. The properties adopted are listed in Tab. 1 and correspond to carbonate rocks tested in the laboratory [11]. The mesh is composed of 8-node quadrilateral elements and nine-point Gauss integration. The model is initialized with isotropic stress state (σ_c) of 10 MPa. The damage zones are created by the incremental application of displacement

at part of the model bottom and at its the right lateral side. Such displacements are at 45° with the vertical direction. The horizontal displacements on the left side of the model are restricted in the horizontal direction. At the bottom, where no prescribed displacements are imposed, we consider a line that represents a rigid plate that is used to avoid the excessive distortion of some elements close to the region where the displacements are imposed.

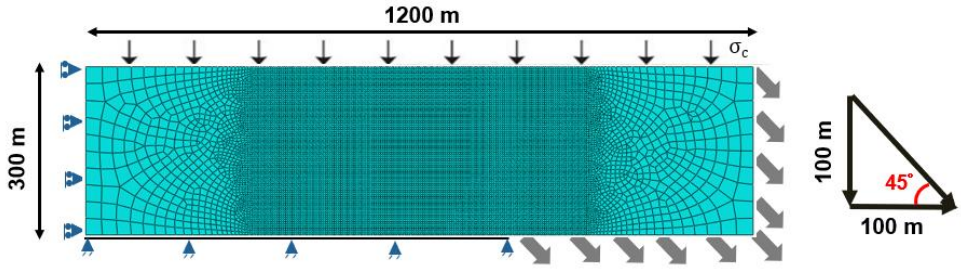

Figure 2. Geometry, mesh and boundary conditions of finite element models.

Table 1. Properties of the carbonate rock [11]

Constitutive relation	Nomenclature	Value
Young's modulus (GPa)	E	17.0
Poisson's ratio (-)	ν	0.3
Friction angle (°)	Φ	34°
Cohesion (MPa)	C	6
Dilation angle (°)	ψ	24°

The simulations were carried out using the Abaqus/Standard® solver considering a large displacement formulation. In each simulation, we assume that the damage zones correspond to those regions that trigger plastic deformations. In fact, the plastic region of the model is equivalent to the fault zone as a whole. However, the plastic zone can be considered, as an approximation, as the damage zone, since the core depends on other different factors and is not always formed.Therefore, we use a scalar variable (PEMAG) that represents the magnitude of plastic regions. Such parameter is defined through:

$$PEMAG = \sqrt{2/3(PE_{P1}{}^2 + PE_{P2}{}^2 + PE_{P3}{}^2)} \tag{1}$$

where PE_{P1}, PE_{P2} and PE_{P3} are the principal plastic strains.

In order to measure the damage zone width, a horizontal path is included in the model, as shown in Fig. 3. Over this path, we obtain the PEMAG distribution at each step of the simulations. The limit of the damage zone is defined by the inflection point of the PEMAG distribution curve, which is approximately equal to 0.25, as shown on the right side of Fig. 3.

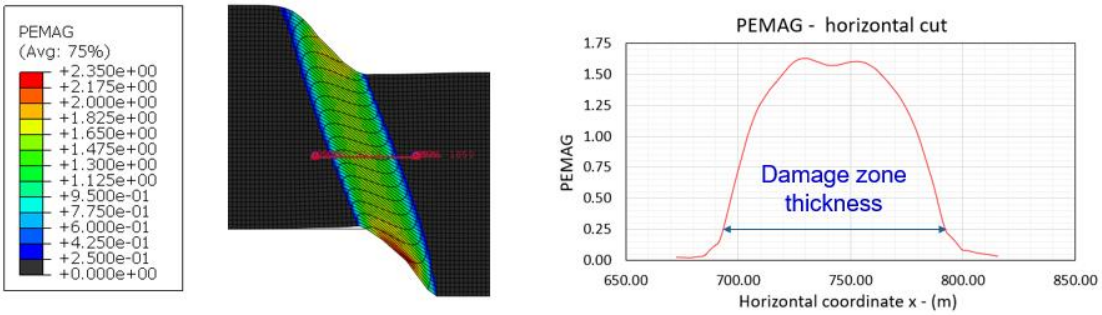

Figure 3. Measurement of the damage zone width.

3 Results

The use of the FEM may lead to mesh-dependent solutions for this kind of problem. Thus, we perform a mesh sensitivity study considering different element sizes with edges length of 4, 6, 9 and 12 m at the central region of the model, where the damage zone develops. For each model, a curve that relates the damage zone width (W) to the imposed vertical displacement (D), in a similar way as field observations, are registered. Figure 4 shows the obtained curves considering all meshes. As it can be noticed, for a given displacement, the damage zone width increases with the element size. However, there is a convergence of results when element sizes are lower than 6 m. Therefore, for further sensitivity analyses, we adopt a mesh with element sizes of 6 m in the central region of the model. That mesh has 19378 nodes and 6283 quadrilateral elements.

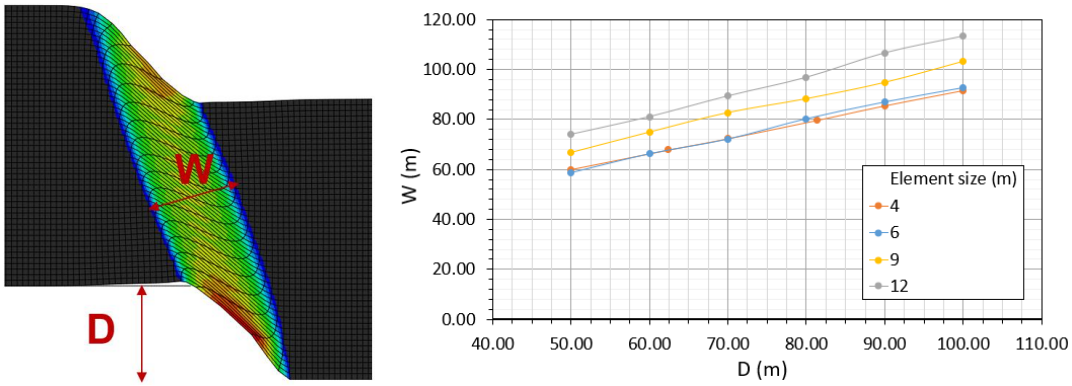

Figure 4. Results obtained in the mesh sensitivity study.

The results considering the material properties listed in Tab. 1 are shown in Fig. 5. For comparison purposes, those numerical results are plotted together with outcrop observations registered in carbonate rock [4][9][10].. We can see that the numerical results are very close to a power-law relation obtained, considering all field observations.

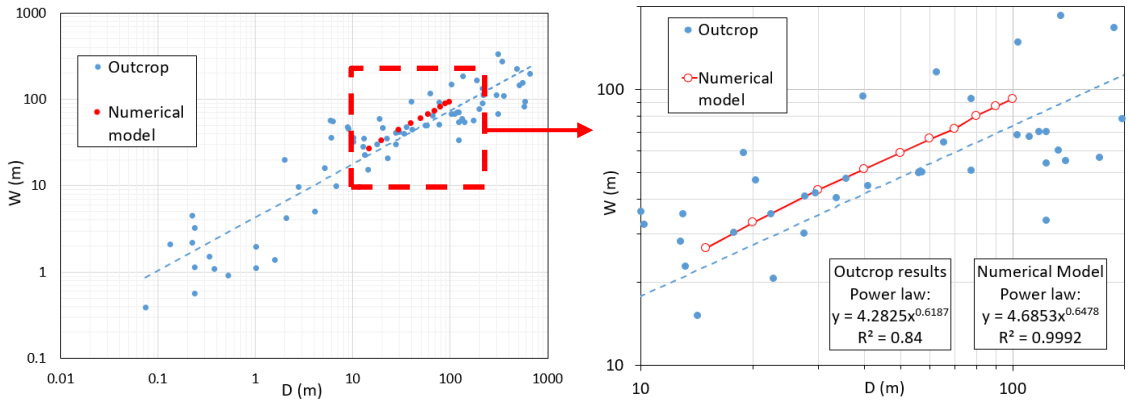

Figure 5. Comparison between outcrop test results and numerical model results.

Then, we performed a sensitivity study to check the influence of each parameter on the development of damage zones. In total, we perform five sets of simulations varying the parameters of Tab. 1 one per time while the others remain fixed.

In the first and second sets of simulations, we vary the elastic parameters: Young's modulus and Poisson's ratio. The corresponding results DxW are shown in Fig. 6. From the variation of Young's modulus, we notice some differences only for the least stiffness, obtaining lower damage zone widths (in the order of 1-2 m) for low displacements. However, for stiffer rocks and large displacements, such differences are imperceptible. From the Poisson ratio variation, we observe that this parameter does not affect the damage zone width.

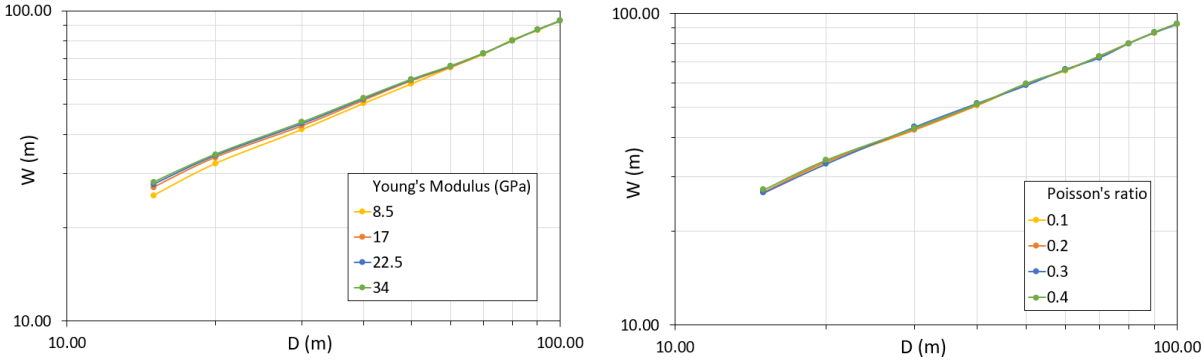

Figure 6. Band width results by varying Young's modulus (left) and Poisson's ratio (right).

In the following test sets, we evaluate the influence of the strength parameters: friction angle and cohesion. The results obtained varying the friction angle are shown on the left side of Fig. 7. We notice that the friction angle has a significant impact on the development of damage zones. For displacements of 100 m, for example, we see that the damage zone widths with friction angles of 24° and 38° present differences up to 30 m. Those results are expected since higher friction angles delay the occurrence of plastic deformations according to the Mohr-Coulomb criterion. Hence, the damage zone width is higher for low friction angles. From the cohesion variation, on the right of Fig. 7, we can notice that such a parameter affects the damage zone only for small displacements. However, for displacements up to 30 m, the cohesion does not seem to affect the damage zone width.

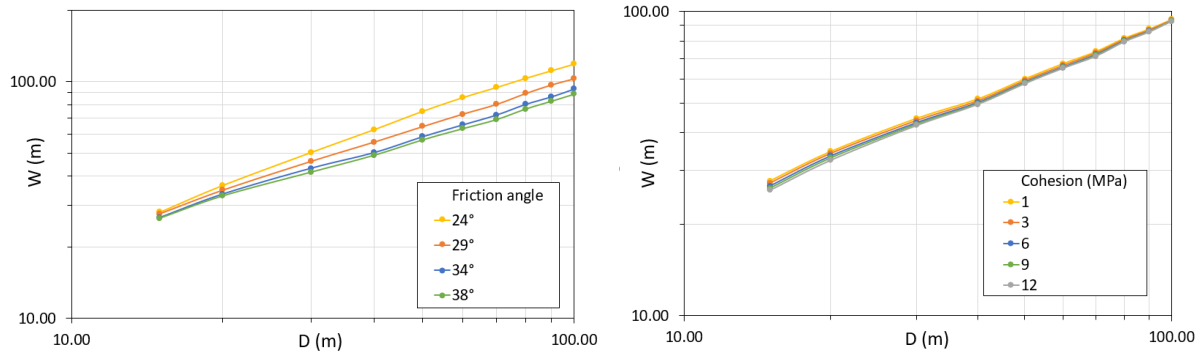

Figure 7. Band width results by varying the friction angle (left) and cohesion (right).

We also perform a set of tests varying the dilation angle, always with values lower or equal than the friction angle, fixed at 34°. The obtained results are shown in Fig. 8. We can notice that the dilatation angle has a major impact on the damage zone, not only the width but also on the inclination angle of the band. From the figure on the left of Fig. 8, we can see that lower dilation angles trigger lower damage zone widths. Those results are expected since lower dilation angles limit the occurrence of volumetric plastic deformations. From the right side of Fig. 8, we can see that the inclination angle of the formed band is approximately the sum of both angles, the inclination of the imposed displacement (45°), and the adopted dilation angle.

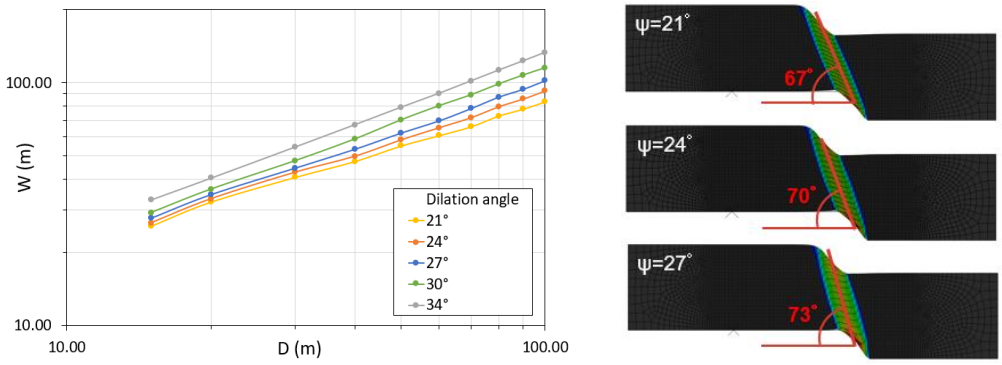

Figure 8. Band width and inclination according to the dilatation angle.

In further simulations, we evaluate the impact of the initial stresses on the development of damage zones. On the left of Fig. 9, we see the results considering different values of isotropic stresses. We observe that for lower displacements, the damage zone width is larger for lower initial stresses. These results are expected since higher stress states are more distant from the Mohr-coulomb envelope, delaying the occurrence of plastic deformations at the beginning of the simulations. However, for larger displacements, the initial stress does not seem to affect the results. In another set of tests, we fixed the vertical stress in 10 MPa and initialized the horizontal stresses considering different horizontal stress ratios. The results are illustrated on the right side of Fig. 9. It seems that the horizontal stress does not affect the damage zone evolution.

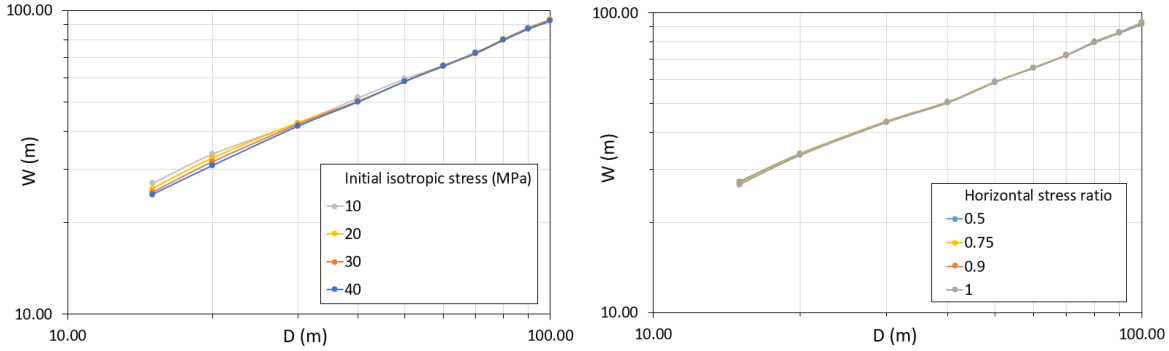

Figure 9. Band width results by varying the initial isotropic stress (left) and the horizontal stress ratio (right).

4 Conclusions

In this study, we present a sensitivity analysis for the characterization of damage zones in carbonate rocks at a reservoir scale. For such purpose, we carry out numerical simulations considering FEM and a Mohr-Coulomb failure criterion with a non-associative flow rule. Initially, we perform a mesh sensitivity study that showed that the results are dependent on the finite element size. However, by reducing the element size, results converged, being possible to define a suitable element size. Several sets of simulations were carried out, aiming to identify the impact of elastic and strength properties in the development of damage zones, which are characterized by widths and vertical displacements measured in the tests. From the obtained results, neither the cohesion nor the elastic properties seem to be relevant properties for the development of damage zones.

On the other hand, we observed that both friction and dilation angles have a direct impact on the damage zone. From tests varying the friction angle, we confirmed that for higher friction angles, the damage zone width is smaller. Such an impact is the opposite in the case of the dilation angle. For greater dilation angles, the damage zone width is higher. In a final set of tests, we also evaluate the influence of the initial stresses. The results showed that the initial stresses have some influence when the vertical displacements are low, leading to broader damage zones when lower stresses are considered. Moreover, we show that the numerical results agree with outcrop observations and show that numerical modeling can be an excellent tool for damage zones characterization.

Finally, it is important to mention that this research follows up at Tecgraf Institute at PUC-Rio, aiming at considering other essential features such as hardening and/or softening material response, plastic compaction, and the behavior at different scales.

Acknowledgements. This research was carried out in association with the ongoing R&D project registered as ANP n° 21475-9, "GeoBand – Geomodelagem de zona de dano em falhas geológicas" (PUC-Rio/CENPES/ANP), sponsored by Petrobras. The authors also gratefully acknowledge the support from Fundação de Amparo à Pesquisa do Rio de Janeiro (FAPERJ) Grant E-26/200.216/2020.

Authorship statement. The authors hereby confirm that they are the sole liable persons responsible for the authorship of this work, and that all material that has been herein included as part of the present paper is either the property (and authorship) of the authors, or has the permission of the owners to be included here.

References

[1] M. D. Zoback, *Reservoir Geomechanics*. Cambridge University Press, 2010.
[2] H. Fossen, *Structural Geology*. Cambridge University Press, 2010.
[3] A. Torabi, M. U. Johannessen, and T. S. S. Ellingsen, "Fault core thickness: Insights from siliciclastic and carbonate rocks," *Geofluids*, vol. 2019, 2019.
[4] S. Mayolle *et al.*, "Scaling of fault damage zones in carbonate rocks," *J. Struct. Geol.*, vol. 124, no. April, pp. 35–50, 2019.
[5] A. Torabi, T. S. S. Ellingsen, M. U. Johannessen, B. Alaei, A. Rotevatn, and D. Chiarella, "Fault zone architecture and its scaling laws: where does the damage zone start and stop?," *Geol. Soc. London, Spec. Publ.*, pp. SP496-2018–151, 2019.
[6] J. Rohmer, T. K. Nguyen, and A. Torabi, "Off-fault shear failure potential enhanced by high-stiff/low-permeable damage zone during fluid injection in porous reservoirs," *Geophys. J. Int.*, vol. 202, no. 3, pp. 1566–1580, 2015.
[7] J. H. Choi, P. Edwards, K. Ko, and Y. S. Kim, "Definition and classification of fault damage zones: A review and a new methodological approach," *Earth-Science Rev.*, vol. 152, pp. 70–87, 2016.
[8] S. S. Berg and T. Skar, "Controls on damage zone asymmetry of a normal fault zone: Outcrop analyses of a segment of the Moab fault, SE Utah," *J. Struct. Geol.*, vol. 27, no. 10, pp. 1803–1822, 2005.
[9] B. Alaei and A. Torabi, "Seismic imaging of fault damaged zone and its scaling relation with displacement," *Interpretation*, vol. 5, no. 4, pp. 83-SP93, 2017.
[10] F. Balsamo *et al.*, "Anatomy and paleofluid evolution of laterally restricted extensional fault zones in the jabal qusaybah anticline, salakh arch, oman," *Bull. Geol. Soc. Am.*, vol. 128, no. 5–6, pp. 957–972, 2016.
[11] M. C. D. Kiewiet, "Comportamento hidromecanico de zonas de falha em travertino: Estudo Experimental e Numérico sobre o Impacto da Reativação Estrutural na Produção de Reservatórios". PhD thesis, Universidade Federal do Rio de Janeiro – UFRJ, 2015.
[12] S. J. H. Buiter *et al.*, "The numerical sandbox: Comparison of model results for a shortening and an extension experiment," *Geol. Soc. Spec. Publ.*, vol. 253, pp. 29–64, 2006.
[13] G. G. Gray, J. K. Morgan, and P. F. Sanz, "Overview of continuum and particle dynamics methods for mechanical modeling of contractional geologic structures," *J. Struct. Geol.*, vol. 59, pp. 19–36, 2014.
[14] I. Anastasopoulos, G. Gazetas, M. F. Bransby, M. C. R. Davies, and A. El Nahas, "Fault Rupture Propagation through Sand: Finite-Element Analysis and Validation through Centrifuge Experiments," *J. Geotech. Geoenvironmental Eng.*, vol. 133, no. 8, pp. 943–958, 2007.